

Information gain at the onset of habituation to repeated stimuli

Giorgio Nicoletti,^{1,2,3} Matteo Bruzzone,^{4,5} Samir Suweis,^{2,5} Marco Dal Maschio,^{4,5} and Daniel Maria Busiello⁶

¹*ECHO Laboratory, École Polytechnique Fédérale de Lausanne, Lausanne, Switzerland*

²*Laboratory of Interdisciplinary Physics, Department of Physics and*

Astronomy “Galileo Galilei”, University of Padova, Padova, Italy

³*Department of Mathematics “Tullio Levi-Civita”, University of Padova, Padova, Italy*

⁴*Department of Biomedical Science, University of Padova, Padova, Italy*

⁵*Padova Neuroscience Center, University of Padova, Padova, Italy*

⁶*Max Planck Institute for the Physics of Complex Systems, Dresden, Germany*

Biological and living systems process information across spatiotemporal scales, exhibiting the hallmark ability to constantly modulate their behavior to ever-changing and complex environments. In the presence of repeated stimuli, a distinctive response is the progressive reduction of the activity at both sensory and molecular levels, known as habituation. Here, we solve a minimal microscopic model devoid of biological details to show that habituation is driven by negative feedback provided by a slow storage mechanism. Crucially, an intermediate level of habituation is associated with a steep increase in the information that the system collects on the external input over time. We find that the region characterized both by maximal information gain and by the onset of habituation can be retrieved if the system tunes its parameters to minimize dissipation and maximize information at the same time. We test our dynamical predictions against experimentally recorded neural responses in a zebrafish larva subjected to repeated looming stimulation. Our work makes a fundamental step towards uncovering the core mechanisms that shape habituation in biological systems, elucidating its information-theoretic and functional role.

Sensing, adaptation, and habituation mechanisms in biological systems span a wide range of temporal and spatial scales, from cellular to multi-cellular level, forming the basis for decision-making and the optimization of limited resources [1–8]. Prominent examples include the modulation of flagellar motion operated by bacteria according to changes in the local nutrient concentration [9–11], the regulation of immune responses through feedback mechanisms [12, 13], the progressive reduction of neural activity in response to repeated looming stimulation [14–16], and the maintenance of high sensitivity in varying environments for olfactory or visual sensing in mammalian neurons [17–21].

In the last decade, advances in experimental techniques fostered the quest for the core biochemical mechanisms governing information processing. Simultaneous recordings of hundreds of biological signals made it possible to infer distinctive features directly from data [22–25]. However, many of these approaches fall short of describing the connection between the underlying chemical processes and the observed behaviors [26–29]. To fill this gap, several works focused on the architecture of specific signaling networks, from tumor necrosis factor [12, 13] to chemotaxis [9, 30], highlighting the essential structural ingredients for their efficient functioning. An observation shared by most of these studies is the key role of a negative feedback mechanism to induce emergent adaptive responses [31–34]. Moreover, any information-processing system, biological or not, must obey information-thermodynamic laws that prescribe the necessity of a storage mechanism [35]. This is an unavoidable feature of numerous chemical signaling networks [9, 31] and biochemical realizations of Maxwell Demons [36, 37]. The storage of information consumes energy during processing [38, 39], and thus

general sensing mechanisms have to take place out-of-equilibrium [3, 40–42]. Recently, the discovery of memory molecules [43–45] hinted at the implementation of storing mechanisms directly at the molecular scale. Overall, negative feedback, storage, and out-of-equilibrium conditions seem to be necessary requirements for a system to process environmental information and act accordingly. To quantify the performance of a biological information-processing system, theoretical developments made substantial progress in highlighting thermodynamics limitations and advantages [17, 46, 47], making a step towards linking information and dissipation from a molecular perspective [36, 48, 49].

In this work, we consider an archetypal model for sensing that encapsulates all these key ingredients, i.e., negative feedback, storage, and energy dissipation, and study its response to repeated stimuli. Indeed, in the presence of dynamic environments, it is common for a biological system to keep encountering the same stimulus. Under these conditions, a progressive decay in the amplitude of the response is often observed, both at sensory and molecular levels. In general terms, such adaptive behavior is usually named *habituation* and it is a common phenomenon, from biochemical concentrations [50–52] to populations of neurons [14–16, 53, 54]. Despite its ubiquity, the onset of habituation from general microscopic models remains unexplored, along with its functional advantages in terms of information gain and energy dissipation.

In this work, we tackle these questions. Our architecture is inspired by those found in real biological systems operating at different scales [12, 17] and resembles the topologies of minimal networks exhibiting adaptive features in different contexts [50, 51, 55]. By deriving the

exact solution of this prototypical model, we identify that the key mechanism driving habituation is the negative feedback provided by slow information storage. We find that the information gain over time peaks at intermediate levels of habituation, uncovering that optimal processing performances are not necessarily tangled with maximal activity reduction. This optimal region can be retrieved by simultaneously minimizing dissipation and maximizing information, hinting at an a priori optimal region of operation for biological systems. Our results open the avenue to understanding the emergence of habituation, along with its information-theoretic advantage.

RESULTS

Archetypal model for sensing in biological systems

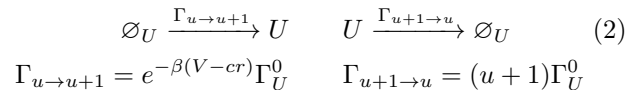
We describe a model with three fundamental units: a receptor (R), a readout population (U), and a storage population (S) (Figure 1a). The presence of these three distinct components is a feature shared by several topologies exhibiting adaptive responses of various kinds [30, 50, 51, 55]. The role of the receptor is to sense external inputs, which we represent as a time-varying environment (H) described by the probability distribution $p_H(h, t)$. The receptor can be either active ($r = 1$) or passive ($r = 0$), with the two states separated by an energetic barrier, ΔE . A strong external signal favors activation of the receptor, while inhibition takes place through a negative feedback process mediated by the concentration of the storage, $[S]$. The negative feedback acts to reduce the level of activity of the system, and its effect on the receptor resembles known motifs found in biochemical systems (see Figure 1b-e) [12, 17]. We model the activation of the receptor by the environmental signal through a ‘‘sensing pathway’’ (superscript H). Instead, the inhibition mechanism affects an ‘‘internal pathway’’ of reactions (superscript I). By assuming that the rates follow an effective Arrhenius’ law, we end up with:

$$\begin{aligned} \Gamma_{P \rightarrow A}^{(H)} &= e^{\beta(h - \Delta E)} \Gamma_R^0 & \Gamma_{A \rightarrow P}^{(H)} &= \Gamma_R^0 \\ \Gamma_{P \rightarrow A}^{(I)} &= e^{-\beta \Delta E} \Gamma_R^0 & \Gamma_{A \rightarrow P}^{(I)} &= \Gamma_R^0 e^{\beta \kappa [S]} \end{aligned} \quad (1)$$

where $\Gamma_R^0 = \tau_R^{-1}$ sets the timescale of the receptor. For simplicity, the driving induced by inhibition appearing in $\Gamma_{A \rightarrow P}^{(I)}$ depends linearly on the concentration of S at a given time through a proportionality constant κ . Here, the inverse temperature β encodes the thermal noise, as lower values of β are associated with faster reactions (see Methods for a detailed discussion on model parameters). Crucially, the presence of two different transition pathways, motivated by molecular considerations and pivotal in many energy-consuming biochemical systems [36, 56, 57], creates an internal non-equilibrium cycle in receptor dynamics.

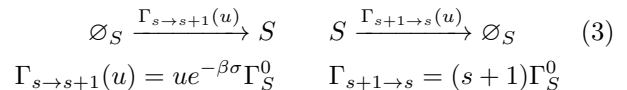
Whenever active, the receptor drives the production of the readout population U , which represents the direct re-

sponse of the system to environmental signals. As such, we consider it to be the observable that characterizes habituation. It may describe, for example, photo-receptors or calcium concentration for olfactory or visual sensing mechanisms [14–16, 18–21]. We model its dynamics with a stochastic birth-and-death process:



where u denotes the number of molecules, $\Gamma_U^0 = \tau_U^{-1}$ sets the timescale of readout production, and V is the energy needed to produce a readout unit. When the receptor is active, $r = 1$, this effective energetic cost is reduced by c by an effective additional driving. Thus, active receptors transduce the environmental energy into an active pumping on the readout node, allowing readout units to encode information on the external signal.

Finally, readout units stimulate the production of the storage population S . Its number of molecules s follows a controlled birth-and-death process [58–60]:



where σ is the energetic cost of a storage unit and Γ_S^0 sets the timescale, i.e., $\Gamma_S^0 = \tau_S^{-1}$. For simplicity, we set a first-order catalytic form for $\Gamma_{s \rightarrow s+1}(u)$ and allow for a maximum number of storage units, N_S , so that $[S] = s/N_S$. The storage may represent different molecular mechanisms at a coarse-grained level as, for example, memory molecules sensitive to calcium activity [43], synaptic depotentiation, and neural populations that regulate neuronal response [14, 15]. Storage units, as we will see, are responsible for encoding the readout response and play the role of a finite-time memory.

Our model, being devoid of specific biological details, can be declined to describe systems at very different scales (Figure 1b-d). We do not expect any detailed biochemical implementation to qualitatively change our results. However, we expect from previous studies [60] that the presence of multiple timescales in the system will be fundamental in shaping information between the different components. Thus, we employ the biologically plausible assumption that U undergoes the fastest evolution, while S and H are the slowest degrees of freedom [30, 61]. We have that $\tau_U \ll \tau_R \ll \tau_S \approx \tau_H$, where τ_H is the timescale of the environment.

The onset of habituation and its functional role

Habituation occurs when the response of the system, represented by the number of active readout units, decreases upon repeated stimulation. In our architecture, we expect it to emerge due to the increase in the storage population, which in turn provides an increasing negative

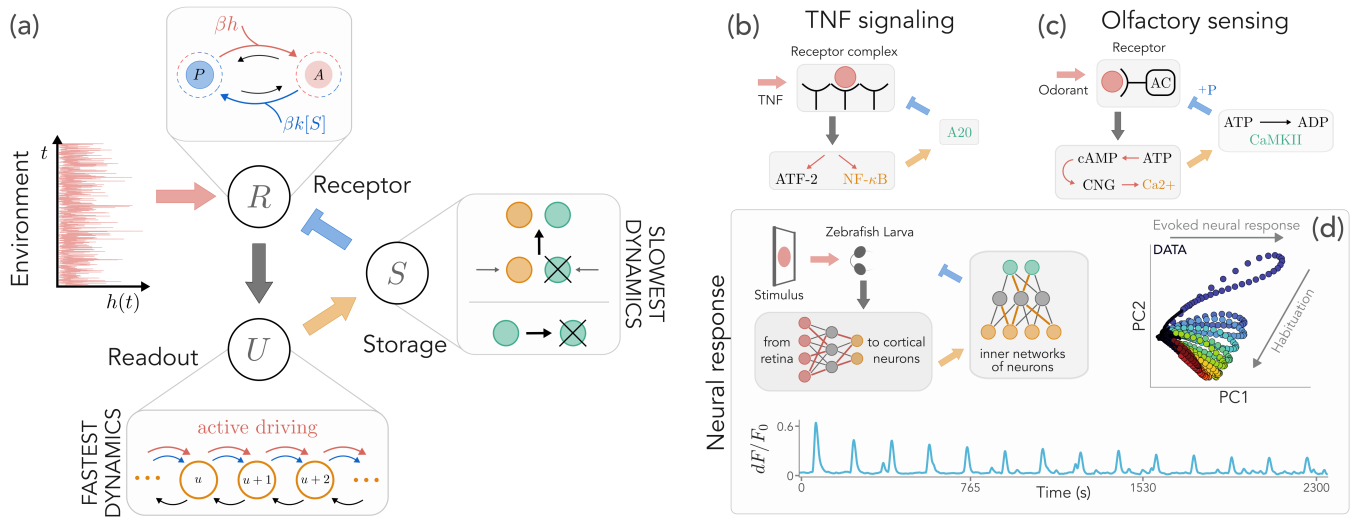


FIG. 1. Sketch of the model architecture and biological examples at different scales. (a) A receptor R transitions between an active (A) and passive (P) state along two pathways, one used for sensing (red) and affected by the environment h , and the other (blue) modified by the storage concentration, $[S]$. An active receptor increases the response of a readout population U (orange), which in turn stimulates the production of storage units S (green) that provide negative feedback to the receptor. (b) In tumor necrosis factor (TNF) signaling, we can identify a similar architecture. The nuclear factor $NF - \kappa B$ is produced after receptor binding to TNF. $NF - \kappa B$ modulates the encoding of the zinc-finger protein A20, which closes the feedback loop by inhibiting the receptor complex. (c) Similarly, in olfactory sensing, odorant binding induces the activation of adenylyl cyclase (AC). AC stimulates a calcium flux, eventually producing phosphorylase calmodulin kinase II (CAMKII) which phosphorylates and deactivates AC. (d) In neural response, multiple mechanisms take place at different scales. In zebrafish larvae, visual stimulation is projected along the visual stream from the retina to the cortex, a coarse-grained realization of the R - U dynamics. Neural habituation emerges upon repeated stimulation, as measured by calcium fluorescence signals (dF/F_0) and by the corresponding 2-dimensional PCA of the activity profiles.

feedback to the receptor. To study the onset and the features of habituation, we consider a switching exponential signal, $p_H(h, t) \sim \exp[-h/\langle H \rangle(t)]$. The time-dependent average $\langle H \rangle$ periodically switches between two values, $\langle H \rangle_{\min}$ and $\langle H \rangle_{\max}$, corresponding to a vanishing signal and strong stimulation of the receptor, respectively. Overall, the system dynamics is governed by four different operators, \hat{W}_X , with $X = R, U, S, H$, one for each population and one for the environment. The resulting master equation is:

$$\partial_t P = \left[\frac{\hat{W}_R(s, h)}{\tau_R} + \frac{\hat{W}_U(r)}{\tau_U} + \frac{\hat{W}_S(u)}{\tau_S} + \frac{\hat{W}_H}{\tau_H} \right] P, \quad (4)$$

where P denotes, in general, the joint propagator $P(u, r, s, h, t | u_0, r_0, s_0, h_0, t_0)$, with u_0, r_0, s_0 and h_0 initial conditions at time t_0 . By taking advantage of the timescale separation, we can write an exact self-consistent solution to Eq. (4) at all times t (see Methods and Supplementary Information).

We assume that $\langle H \rangle$ switches to $\langle H \rangle_{\max}$ at equally spaced intervals t_1, \dots, t_N , each with the same duration ΔT . After a large number of inputs, the system reaches a time-periodic steady-state (see Fig. 2d-e). Thus, habituation is quantified by the change in the average response of the system:

$$\Delta \langle U \rangle = \langle U \rangle(t_\infty) - \langle U \rangle(t_1) \quad (5)$$

where t_1 is the time of the first signal, and t_∞ is the time of a signal at the steady state. Whenever $\Delta \langle U \rangle < 0$, the system is habituating to the external inputs. In Figure 2a, we study habituation as a function of the inverse temperature β and the energetic cost of storage, σ (see Methods). As expected, habituation is stronger at small σ , where a large storage production provides a strong negative feedback to the receptor, sharply decreasing $\langle U \rangle$.

During its dynamical evolution, the system encodes information on the environment H . We are particularly interested in how much information is captured by the readout population, which is measured by the mutual information between U and H at time t (see Methods):

$$I_{U,H}(t) = \mathcal{H}[p_U](t) - \int_0^\infty dh p_H(h, t) \mathcal{H}[p_{U|H}](t) \quad (6)$$

where $\mathcal{H}[p](t)$ is the Shannon entropy of the probability distribution p , and $p_{U|H}$ denotes the conditional probability distribution of U given H . $I_{U,H}$ quantifies the system performance in terms of the information that the readout population captures on the external input at each time. Furthermore, it coincides with the entropy increase of the readout distribution:

$$k_B I_{U,H} = -k_B (\mathcal{H}[p_{U|H}] - \mathcal{H}[p_U]) = -\Delta S_U. \quad (7)$$

In Figure 2b, we show how the corresponding information gain $\Delta I_{U,H}$, defined in analogy to Eq. (5), changes

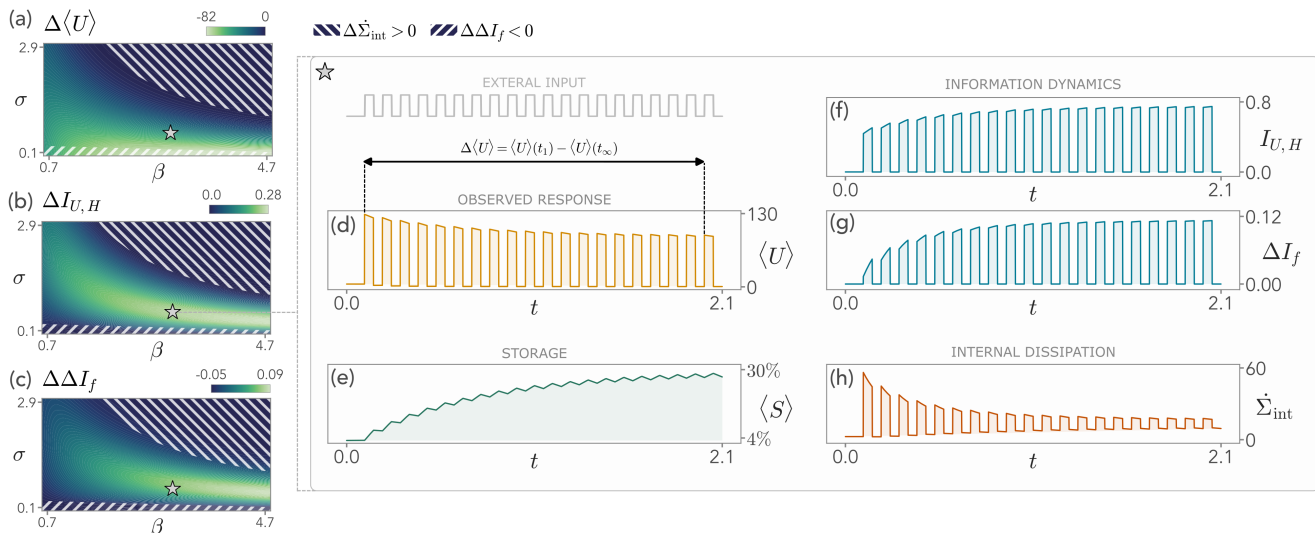


FIG. 2. Evolution of the model under a switching external field $H(t)$. (a) The change in the average readout population $\Delta \langle U \rangle$ between the first signal and after a large number of signals, as a function of the inverse temperature β and the energetic cost of storage σ . $\Delta \langle U \rangle$ quantifies the habituation strength. (b) The change in the mutual information between the readout population and the external field, $\Delta I_{U,H}$. A region with maximal information gain corresponds to intermediate habituation strength. (c) The change in the feedback information $\Delta \Delta I_f$ indicates that, close to the region of maximal information gain, the storage favors information. (d-e) In the region of maximal information gain, the average number of readout units, $\langle U \rangle$, decreases with the number of repetitions, while the average storage concentration, $\langle S \rangle$, increases. At large times, the system reaches a periodic steady state. (f-g) In the same region, the information encoded on H through the readout, $I_{U,H}$, increases in time during habituation, boosting in turn the feedback information, ΔI_f . (h) The internal dissipation rate due to the production of U and S , $\dot{\Sigma}_{\text{int}}$, decreases in time. Model parameters for panels (d-h) are $\beta = 3$, $\sigma = 0.6$ (in the unit measure of energy, for simplicity), and as specified in the Methods.

with β and σ . We find a region where the information gain is maximal. Surprisingly, this region corresponds to intermediate values of $\Delta \langle U \rangle$, suggesting that strong habituation driven by a low energetic cost of storage is ultimately detrimental to the system.

We can understand this feature by introducing the feedback information

$$\Delta I_f = I_{(U,S),H} - I_{U,H} > 0 \quad (8)$$

which quantifies how much the simultaneous knowledge of U and S increases $I_{U,H}$ with respect to knowing solely U . We find that, during repeated external stimulation, the change in feedback information $\Delta \Delta I_f$, again in analogy to Eq. (5), may be negative (Figure 2c). This indicates that the negative feedback on the receptor is impeding the information-theoretic performances of the system, independently of the habituation strength. Crucially, $\Delta \Delta I_f$ sharply increases in the region of maximal information gain, hinting that, at intermediate values of habituation, the information gain in the readout is driven by the storage mechanism. For the sake of simplicity, and to emphasize the information-theoretic advantage, we refer to this region of maximal information gain and intermediate habituation as the “onset” of habituation.

In Figure 2(d-g), we show the evolution of the system for values of (β, σ) that lie in the region of maximal information gain. The readout activity decreases in time,

modulating the response of the system to the repeated input (Figure 2d). This behavior resembles recent observations on habituation under analogous external conditions in various experimental systems [14, 15, 50–52]. We emphasize that the readout population is the fastest species at play, hence each point of the trajectory $\langle U \rangle(t)$ corresponds to a steady-state solution. As expected, the reduction of $\langle U \rangle$ is a direct consequence of the increase of the average storage population, $\langle S \rangle$ (Figure 2e). In this region, both the increase of $I_{U,H}$ and ΔI_f over time during habituation are optimal (Figure 2f). This behavior may seem surprising, since the increase in $I_{U,H}$ is concomitant to a reduction of the population that is encoding the signal. However, let us note that the mean of U is not directly related to the factorizability of the joint distribution $p_{U,H}$, i.e., to how much information on the signal is encoded in the readout. Furthermore, the inhibitory effect provided by S is enhanced by repeated stimuli, generating a stronger dependency between H and U over time.

The increase of $I_{U,H}$ comes along with another intriguing result. Since during habituation, the concentrations of the internal populations U and S change in time, we can quantify how much energy is required to support these processes. The rate of dissipation into the environ-

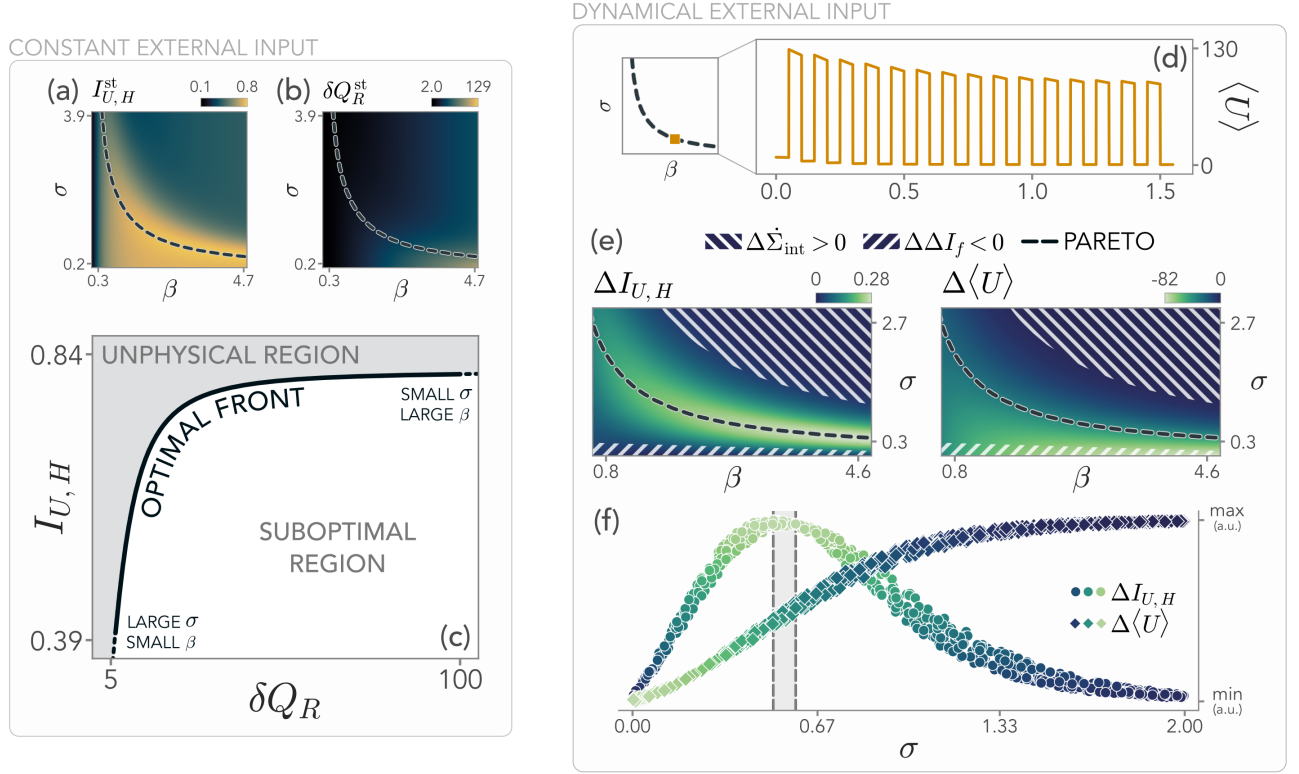


FIG. 3. Optimality at the onset of habituation. (a-b) Contour plots in the (β, σ) plane of the stationary mutual information $I_{U,H}^{st}$ and the receptor dissipation per unit temperature, δQ_R^{st} , in the presence of a constant external input. (c) For a given value of β , the system can optimize σ to the Pareto front (black line) to simultaneously minimize δQ_R and maximize $I_{U,H}$. Each point in this space corresponds to a different strategy γ . If $\gamma = 0$, the system minimizes dissipation only, and if $\gamma = 1$ it only maximizes information. Below the front, the system exploits the available energy suboptimally, reaching lower values of information. In contrast, the region above the front is physically inaccessible. (d-e) In the presence of a dynamical input, the parameters defining the optimal front capture the region of maximal information gain and thus correspond to the onset of habituation, where $\langle U \rangle$ starts to be significantly smaller than zero. (f) Projection of $\Delta I_{U,H}$ and $\Delta \langle U \rangle$ along σ for a range of values of $\beta \in [3 - 3.5]$. The gray area enclosed by the dashed vertical lines indicates the location of the Pareto front for these values. $\Delta I_{U,H}$ clearly peaks at optimality, while $\Delta \langle U \rangle$ takes intermediate values.

ment due to these internal mechanisms is (see Methods):

$$\dot{\Sigma}_{\text{int}} = \sum_{u,s} \left(\Gamma_{s \rightarrow s+1} p_{U,S}(u,s,t) + \right. \quad (9)$$

$$\left. - \Gamma_{s+1 \rightarrow s} p_{U,S}(u,s+1,t) \right) \log \frac{\Gamma_{s \rightarrow s+1}}{\Gamma_{s+1 \rightarrow s}}.$$

We refer to $\dot{\Sigma}_{\text{int}}$ as the internal dissipation of the system and, in Figure 2h, we show that it decreases over time, hinting at a synergistic thermodynamic advantage the onset of habituation.

Maximal information gain from an optimization principle

We now investigate whether the region of maximal information gain can be retrieved by means of an a priori optimization principle. To do so, we focus on the case of a constant environment. In this scenario, the

system can tune its internal parameters to optimally respond to the statistics of an external input during a prolonged stimulation, i.e., the system “learns” the parameters while measuring an input with a large (infinite) observation time. Thus, the input statistics is given by $p_H^{st}(h) \sim \exp[-h/\langle H \rangle_{\text{max}}]$.

When the system reaches its steady state, the information that the readout has on the signal, $I_{U,H}^{st}$, is estimated from the joint probability $p_{U,S,R,H}^{st}$ (Figure 3a). At the same time, however, the system is consuming energy to maintain the receptor active. The receptor dissipation per unit temperature is given by

$$\delta Q_R = \left\langle \log \left(\frac{\Gamma_{P \rightarrow A}^{(H)} \Gamma_{A \rightarrow P}^{(I)}}{\Gamma_{A \rightarrow P}^{(H)} \Gamma_{P \rightarrow A}^{(I)}} \right) \right\rangle = \beta \left(\langle H \rangle + \kappa \sigma \frac{\langle S \rangle}{N_S} \right),$$

as we show in Figure 3b. Large values of the mutual information compatible with minimal dissipation in the receptor can be obtained by maximizing the Pareto func-

tional [62]:

$$\mathcal{L}(\beta, \sigma) = \gamma \frac{I_{U,H}(\beta, \sigma)}{\max(I_{U,H})} - (1 - \gamma) \frac{\delta Q_R(\beta, \sigma)}{\max(\delta Q_R)} \quad (10)$$

where $\gamma \in [0, 1]$ sets the strategy implemented by the system. If $\gamma \ll 1$, the system prioritizes minimizing dissipation, whereas if $\gamma \approx 1$ it acts to preferentially maximize information. The set of (β, σ) that maximize Eq. (10) defines a Pareto optimal front in the $(\delta Q_R, I_{U,H})$ space (Figure 3c). At fixed receptor dissipation, this front represents the maximum information between the readout and the external input that can be achieved. The region below the front is therefore suboptimal. Instead, the points above the front are inaccessible, as higher values of $I_{U,H}$ cannot be attained without increasing δQ_R . We note that, since β usually cannot be directly controlled by the system, the Pareto front indicates the optimal σ to which the system tunes at fixed β (see Methods and Supplementary Information for details).

Along this optimal front, we find that the system displays habituation (see Figure 3d). Furthermore, when plotted in the (β, σ) plane in the presence of a switching dynamical input, the front qualitatively corresponds to the region of maximal information gain and the onset of habituation, as we see in Figure 3e. Remarkably, this implies that once the system tunes its internal parameters to respond to a constant signal to maximize information and minimize dissipation, it also learns to respond optimally to the time-varying input in terms of information gain. In Figure 3f, we show that at fixed β , the Pareto front (gray area) represents the region around the peak of $\Delta I_{U,H}$, where $\Delta \langle U \rangle$ attains intermediate values. In other words, the onset of habituation emerges spontaneously when the system attempts to activate its receptor as little as possible, while retaining information about the external environment.

The role of information storage

The presence of a storage mechanism is fundamental in our model. Furthermore, its role in mediating the negative feedback is suggested by several experimental and theoretical observations [9, 30–34]. Crucially, whenever the storage is eliminated from our model, habituation cannot take place, highlighting its key role in driving the observed dynamics.

In Figure 4a, we show that habituation and the change in the storage, $\Delta \langle S \rangle$, are deeply related to one another. The more $\langle S \rangle$ relaxes between two consecutive signals, the less the readout population reduces its activity. This ascribes to the storage population the role of an effective memory and highlights its dynamical importance for habituation. Moreover, the dependence of the storage dynamics on the interval between consecutive signals, ΔT , influences information gain as well. Indeed, increasing ΔT , we observe a decrease of the mutual information (Figure 4b) on the next stimulus, and the system needs

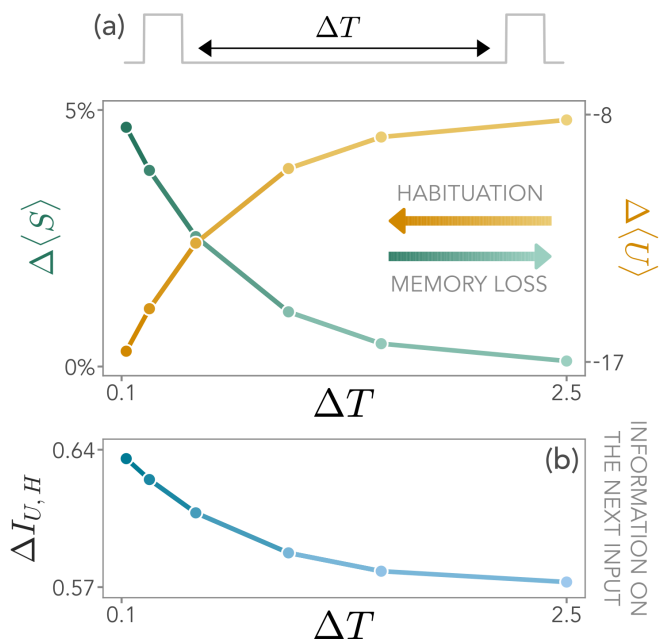


FIG. 4. The role of memory in shaping habituation. (a) The system response depends on the waiting time ΔT_{pause} between two external signals. As ΔT_{pause} increases, the storage decays and thus memory is lost (green), and consequently the habituation of the readout population decreases (yellow). (b) As a consequence, the information $I_{U,H}$ that the system has on the field H when the new stimulus arrives decays as well. Model parameters for this figure are $\beta = 2.5$, $\sigma = 0.5$ in the unit measure of the energy, and as specified in the Methods.

to produce a larger number of readout units upon the new input. In the Supplementary Information, we further analyze the impact of different signal and pause durations.

We remark here that the proposed model is fully Markovian in its microscopic components, and the memory that governs readout habituation spontaneously emerges from the interplay among the internal timescales. In particular, recent works have highlighted that the storage needs to evolve on a slower timescale, comparable to that of the external input, in order to generate information in the receptor and in the readout [60]. In our model, instantaneous negative feedback implemented directly by U (bypassing the storage mechanism) leads to no time-dependent modulations (see Supplementary Information). Conversely, a readout population evolving on a timescale comparable to that of the signal cannot effectively mediate the negative feedback on the receptor since its population increase (as for the storage in the complete model) would not lead to habituation (see Supplementary Information). Thus, negative feedback has to be implemented by a separate degree of freedom evolving on a slow timescale.

Minimal features of neural habituation

In neural systems, habituation is typically measured as a progressive reduction of the stimulus-driven neuronal firing rate [14–16, 53, 54]. To test whether our minimal model can be used to capture the typical neural habituation dynamics, we measured the response of zebrafish larvae to repeated looming stimulations via volumetric multiphoton imaging [63]. From a whole-brain recording of ≈ 55000 neurons, we extracted a subpopulation of ≈ 2400 neurons in the optic tectum with a temporal activity profile that is most correlated with the stimulation protocol (see Methods).

Our model can be extended to qualitatively reproduce some features of the progressive decrease in neuronal response amplitudes. We identify each single readout with a subpopulation of binary neurons. A fraction of neurons are randomly turned on each time a readout unit is activated (see Methods). We tune the model parameters, i.e., β and σ , to the onset of habituation. In this way, we can focus on the effects of storage and feedback mechanisms without modeling further biological details. The patterns of the model-generated activity are remarkably similar to the experimental ones (see Figure 5a). A 2-dimensional embedding of the data via PCA (explained variance $\approx 70\%$) reveals that the evoked neural response is described by the first principal direction, while habituation is reflected in the second (Figure 5b). Remarkably, as we see in Figure 5c, this is the case in our minimal model as well, although the neural response is replaced by the switching input on/off dynamics of the input.

CONCLUSIONS

In this work, we considered a minimal architecture that serves as a microscopic and archetypal description of sensing processes across biological scales. Informed by theoretical and experimental observations, our model includes three fundamental mechanisms: a receptor, a readout population, and a storage mechanism that drives negative feedback. We have shown that our model robustly displays habituation under repeated external inputs, a widespread phenomenon in both biochemical and neural systems. We find a regime of parameters of maximal information gain, where habituation drives an increase in the mutual information between external input and the system’s response. Remarkably, the system can spontaneously tune to this region of parameters if it enforces an information-dissipation trade-off. In particular, optimal systems lie at the onset of habituation, characterized by intermediate levels of activity reduction, as both too-strong and too-weak negative feedback are detrimental to information gain. Our results suggest that the functional advantages of the onset of habituation are rooted in the interplay between energy dissipation and information gain.

Although minimal, our model can capture basic fea-

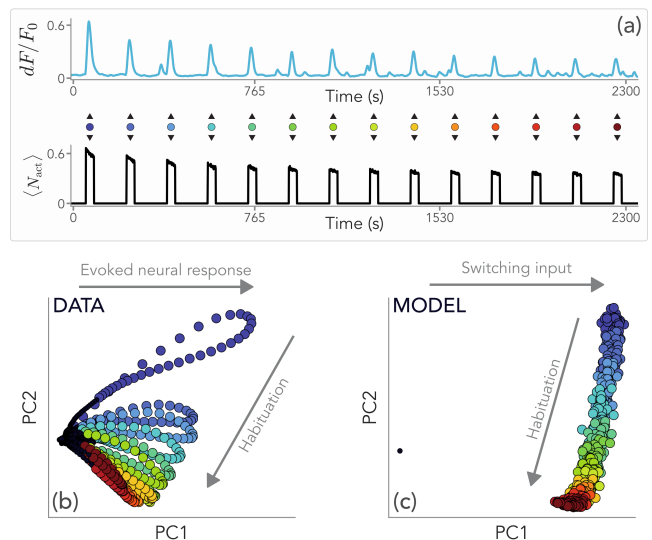


FIG. 5. Habituation in zebrafish larvae. (a) Normalized neural activity profile in a zebrafish larva in response to the repeated presentation of visual stimulation, and comparison with the fraction of active neurons $\langle N_{act} \rangle = N_{act}/N$ in our model with stochastic neural activation (see Methods). Stimuli are indicated with colored dots from blue to red as time increases. (b) PCA of experimental data reveals that habituation is captured mostly by the second principal direction, while features of the evoked neural response by the first one. Different colors indicate responses to different stimuli. (c) PCA of simulated neural activations. Although we cannot capture the dynamics of the evoked neural response with a switching input, the core features of habituation are correctly captured along the second principal direction. Model parameters are $\beta = 3.5$, $\sigma = 0.1$ in energy units, and as in the Methods, so that the system is tuned to the onset of habituation.

tures of neural adaptation, where it is generally accepted that inhibitory feedback mechanisms modulate the stimulus weight [64]. Remarkably, recent works reported the existence of a separate inhibitory neuronal population whose activity increases during habituation [15]. Our model suggests that this population might play the role of a storage mechanism, allowing the system to habituate to repeated signals. Further, recent experiments also showed that by increasing the pause between two consecutive stimuli, the readout starts responding again, in line with our theoretical predictions [15]. This evidence hints at the fact that our minimal architecture may lay the foundation of habituation dynamics across vastly different biological scales.

Extensions of these ideas are manifold. Other *a priori* optimization principles for the system should be considered, focusing in particular on more detailed and realistic molecular schemes. Upon these premises, the possibility of inferring the underlying biochemical structure from observed behaviors is a fascinating direction [50]. Furthermore, since we focused on repetitions of statistically identical signals, it will be fundamental to characterize

the system's response to diverse environments [65]. To this end, incorporating multiple receptors or storage populations may be needed to harvest information in complex conditions. In such scenarios, correlations between external signals may help reduce the encoding effort as, intuitively, S is acting as an information reservoir for the system. However, living systems do not passively read external signals but often act upon the environment. Both storage mechanisms and their associated negative feedback will remain core modeling ingredients, paving the way to understanding how this encoded information guides learning and decision-making, a paramount question in many fields.

Our work serves as a fundamental framework for these ideas. On the one hand, it encapsulates key ingredients to support habituation while still being minimal enough to allow for analytical treatment. On the other hand, it may help the experimental quest for signatures of these physical ingredients in a variety of systems. Ultimately, our results show how habituation - a ubiquitous phenomenon that takes place at strikingly different biological scales - may stem from an information-based advantage, shedding light on the optimization principle underlying its emergence and its relevance for any biological system.

ACKNOWLEDGMENTS

G.N., S.S., and D.M.B. acknowledge Amos Maritan for fruitful discussions. D.M.B. thanks Paolo De Los Rios for insightful comments. G.N. and D.M.B. acknowledge the Max Planck Institute for the Physics of Complex Systems for hosting G.N. during the initial stage of this work.

METHODS

Model parameters. The system is driven out of equilibrium by both the external field and the storage inhibition through the receptor dynamics, whose dissipation per unit temperature is δQ_R . The energetic barrier ($V - cr$) fixes the average values of the readout population both in the passive and active state, namely $\langle U \rangle_P = e^{-\beta V}$ and $\langle U \rangle_A = e^{-\beta(V-c)}$ (see Eq. (2)), and κ controls the effectiveness of the storage in inhibiting the receptor's activation. We assume that, on average, the activation rate due to the field is balanced by the feedback of a fraction $\alpha = \langle S \rangle / N_S$ of the storage population,

$$\left\langle \log \frac{\Gamma_{P \rightarrow A}^{(H)}}{\Gamma_{A \rightarrow P}^{(I)}} \right\rangle = \beta g(\langle H \rangle - \kappa \alpha) = 0 \quad \rightarrow \quad \kappa = \frac{\langle H \rangle}{\alpha},$$

so that we only need to fix α . Moreover, $\Delta E = 1$, $\langle U \rangle_A = 150$, $\langle U \rangle_P = 0.5$, $N_S = 25$, and $\alpha = 2/3$. We remark that the emerging features of the model are independent of the specific choice of these parameters. They affect the number of active units at each time step, but all the results presented here on the information gain during

habituation remain valid. Furthermore, we typically consider the average of the exponentially distributed signal to be $\langle H \rangle_{\max} = 10$ and $\langle H \rangle_{\min} = 0.1$ (see Supplementary Information for details).

Overall, we are left with β and σ as free parameters. β quantifies the amount of thermal noise in the system, and at small β the thermal activation of the receptor hinders the effect of the field and makes the system almost unable to process information. Conversely, if β is high, the system must overcome large thermal inertia, increasing the dissipative cost. In this regime of weak thermal noise, we expect that, given a sufficient amount of energy, the system can effectively process information.

Timescale separation. We solve our system in a timescale separation framework [60, 66, 67], where the storage evolves on a timescale that is much slower than all the other internal ones, i.e.,

$$\tau_U \ll \tau_R \ll \tau_S \approx \tau_H.$$

The fact that τ_S is the slowest timescale at play is crucial to making these components act as an information reservoir. This assumption is also compatible with biological examples. The main difficulty arises from the presence of the feedback, i.e. the field influences the receptor and thus the readout population, which in turn impacts the storage population and finally changes the deactivation rate of the receptor - schematically, $H \rightarrow R \rightarrow U \rightarrow S \rightarrow R$, but the causal order does not reflect the temporal one.

We start with the master equation for the propagator $P(u, r, s, h, t | u_0, r_0, s_0, h_0, t_0)$,

$$\partial_t P = \left[\frac{\hat{W}_U(r)}{\tau_U} + \frac{\hat{W}_R(s, h)}{\tau_R} + \frac{\hat{W}_S(u)}{\tau_S} + \frac{\hat{W}_H}{\tau_H} \right] P.$$

We rescale the time by τ_S and introduce two small parameters to control the timescale separation analysis, $\epsilon = \tau_U/\tau_R$ and $\delta = \tau_R/\tau_H$. Since $\tau_S/\tau_H = \mathcal{O}(1)$, we set it to 1 without loss of generality. We then write $P = P^{(0)} + \epsilon P^{(1)}$ and expand the master equation to find $P^{(0)} = p_{U|R}^{\text{st}}(u|r)\Pi$, with $\hat{W}_U p_{U|R}^{\text{st}} = 0$. We obtain that Π obeys the following equation:

$$\partial_t \Pi = \left[\delta^{-1} \hat{W}_R(s, h) + \hat{W}_S(u) + \hat{W}_H \right] \Pi.$$

Yet again, $\Pi = \Pi^{(0)} + \delta \Pi^{(1)}$ allows us to write $\Pi^{(0)} = p_{R|S,H}^{\text{st}}(r|s, h)F(s, h, t | s_0, h_0, t_0)$ at order $\mathcal{O}(\delta^{-1})$, where $\hat{W}_R p_{R|S,H}^{\text{st}} = 0$. Expanding first in ϵ and then in δ sets a hierarchy among timescales. Crucially, due to the feedback present in the system we cannot solve the next order explicitly to find F . Indeed, after a marginalization over r , we find $\partial_t F = \left[\hat{W}_H + \hat{W}_S(\bar{u}(s, h)) \right] F$, at order $\mathcal{O}(1)$, where $\bar{u}(s, h) = \sum_{u,r} u p_{U|R}^{\text{st}}(u|r) p_{R|S,H}^{\text{st}}(r|s, h)$. Hence, the evolution operator for F depends manifestly on s , and the equation cannot be self-consistently solved. To tackle the problem, we first discretize time, considering a small interval, i.e., $t = t_0 + \Delta t$ with $\Delta t \ll \tau_U$ and

thus $\bar{u}(s, h) \approx u_0$. We thus find $F(s, h, t|s_0, h_0, t_0) = P(s, t|s_0, t_0)P_H(h, t|h_0, t_0)$ in the domain $t \in [t_0, t_0 + \Delta t]$, since H evolves independently from the system (see also Supplementary Information for analytical steps).

$$p_{U,S}(u, t + \Delta t) = \sum_{r=0}^1 \int_0^\infty dh p_{U|R}^{\text{st}}(u|r) p_{R|S,H}^{\text{st}}(r|h, s) p_H(h, t + \Delta t) \sum_{s'=0}^{N_S} \sum_{u'=0}^\infty P(s', t \rightarrow s, t + \Delta t|u') p_{U,S}(u', s', t)$$

where $P(s', t \rightarrow s, t + \Delta t)$ is the propagator of the storage at fixed readout. This is the Chapman-Kolmogorov equation in the timescale separation approximation. Notice that this solution requires the knowledge of $p_{U,S}$ at the previous time-step and it has to be solved iteratively.

Explicit solution for the storage propagator. To find a numerical solution to our system, we first need to compute the propagator $P(s_0, t_0 \rightarrow s, t)$. Formally, we have to solve the master equation

$$\partial_t P(s_0 \rightarrow s|u_0) = \Gamma_S^0 \left[e^{-\beta\sigma} u_0 P(s_0 \rightarrow s') \delta_{s',s-1} + s' P(s_0 \rightarrow s') \delta_{s',s+1} - P(s_0 \rightarrow s') \delta_{s',s} (s' + e^{-\beta\sigma} u_0) \right]$$

where we used the shorthand notation $P(s_0 \rightarrow s) = (s_0, t_0 \rightarrow s, t)$. Since our formula has to be iterated for small time-steps, i.e., $t - t_0 = \Delta t \ll 1$, we can write the propagator as follows

$$P(s_0, t_0 \rightarrow s, t_0 + \Delta t|u_0) = p_{S|U}^{\text{st}} + \sum_{\nu} w_{\nu} a^{(\nu)} e^{\lambda_{\nu} \Delta t}$$

where w_{ν} and λ_{ν} are respectively eigenvectors and eigenvalues of the transition matrix $\hat{W}_S(u_0)$,

$$\begin{aligned} (\hat{W}_S(u_0))_{ij} &= e^{-\beta\sigma} u_0 & \text{if } i = j + 1 \\ (\hat{W}_S(u_0))_{ij} &= j & \text{if } i = j - 1 \\ (\hat{W}_S(u_0))_{ij} &= 0 & \text{otherwise} \end{aligned}$$

and the coefficients $a^{(\nu)}$ are such that

$$p_{S|U}(s_0, t_0 \rightarrow s, t_0 + \Delta t|u_0) = p_{S|U}^{\text{st}} + \sum_{\nu} w_{\nu} a^{(\nu)} = \delta_{s,s_0}.$$

Since eigenvalues and eigenvectors of $\hat{W}_S(u_0)$ might be computationally expensive to find, we employ another simplification. As $\Delta t \rightarrow 0$, we can restrict the matrix only to jumps to the n -th nearest neighbors of the initial state (s_0, t_0) , assuming that all other states are left unchanged in small time intervals. We take $n = 2$ and check that the accuracy of this approximation against the full simulation for a limited number of time-steps.

Iterating the procedure for multiple time steps, we end up with a recursive equation for the joint probability $p_{U,R,S,H}(u, r, s, h, t_0 + \Delta t)$. We are interested in the following marginalization

Mean-field relationship. We note that $\langle U \rangle$ and $\langle S \rangle$ satisfies the following mean-field relationship:

$$\frac{\langle U \rangle - \langle U \rangle_{r=1}}{\langle U \rangle_{r=1} - \langle U \rangle_{r=0}} = f_0 \left(\frac{\langle S \rangle}{N_S} \right), \quad (\text{S1})$$

where $f_0(x)$ is an analytical function of its argument (see Supplementary Information). Eq. (S1) clearly states that only the fraction of active storage units is relevant to determining the habituation dynamics.

Mutual information. Once we have $p_U(u, t)$ (obtained marginalizing $p_{U,S}$ over s) for a given $p_H(h, t)$, we can compute the mutual information

$$I_{U,H}(t) = \mathcal{H}[p_U](t) - \int_0^\infty dh p_H(h, t) \mathcal{H}[p_{U|H}](t)$$

where \mathcal{H} is the Shannon entropy. For the sake of simplicity, we consider that the external field follows an exponential distribution $p_H(h, t) = \lambda(t) e^{-\lambda(t)h}$. Notice that, in order to determine such quantity, we need the conditional probability $p_{U|H}(u, t)$. In the Supplementary Information, we show how all the necessary joint and conditional probability distributions can be computed from the dynamical evolution derived above.

We also highlight here that the timescale separation implies $I_{S,H} = 0$, since

$$\begin{aligned} p_{S|H}(s, t|h) &= \sum_u p_{U,S|H}(u, s, t|h) \\ &= p_S(s, t) \sum_u \sum_r p_{U|R}^{\text{st}}(u|r) p_{R|S,H}^{\text{st}}(r|s, h) \\ &= p_S(s, t). \end{aligned}$$

Although it may seem surprising, this is a direct consequence of the fact that S is only influenced by H through the stationary state of U . Crucially, the presence of the feedback is still fundamental to promote habituation. Indeed, we can always write the mutual information between the field H and both the readout U and the storage S together as $I_{(U,S),H} = \Delta I_f + I_{U,H}$, where $\Delta I_f = I_{(U,S),H} - I_{U,H} = I_{(U,H),S} - I_{U,S}$. Since $\Delta I_f > 0$ (by standard information-theoretic inequalities), the storage is increasing the information of the two populations together on the external field. Overall, although S and H are independent in this limit, the feedback is paramount in shaping how the system responds to the external field and stores information about it.

Dissipation of internal processes The production of readout, u , and storage, s , molecules requires energy. From the modeling of their dynamics as controlled stochastic birth-and-death processes, we quantify the dissipation into the environment using the environmental contribution of the Schnakenberg entropy production, which is also the only one that survives at stationarity [68]. We have:

$$\begin{aligned} \dot{\Sigma}_{\text{int}} = & \sum_{u,s} (\Gamma_{u \rightarrow u+1} p_{U,S}(u, s, h, t) + \\ & - \Gamma_{u+1 \rightarrow u} p_{U,S}(u+1, s, h, t)) \log \frac{\Gamma_{u \rightarrow u+1}}{\Gamma_{u+1 \rightarrow u}} + \\ & + \sum_{u,s} (\Gamma_{s \rightarrow s+1} p_{U,S}(u, s, h, t) + \\ & - \Gamma_{s+1 \rightarrow s} p_{U,S}(u, s+1, h, t)) \log \frac{\Gamma_{s \rightarrow s+1}}{\Gamma_{s+1 \rightarrow s}} \end{aligned}$$

where we indicated all possible dependencies in the joint probability distribution. By employing the timescale separation [66], and noting that $\Gamma_{u \rightarrow u \pm 1}$ do not depend on s , we finally have:

$$\begin{aligned} \dot{\Sigma}_{\text{int}} = & \sum_{u,s} (\Gamma_{s \rightarrow s+1} p_{U,S}(u, s, h, t) + \\ & - \Gamma_{s+1 \rightarrow s} p_{U,S}(u, s+1, h, t)) \log \frac{\Gamma_{s \rightarrow s+1}}{\Gamma_{s+1 \rightarrow s}} \end{aligned}$$

As this quantity decreases during habituation, the system tends to dissipate less and less into the environment to produce the internal populations that are required to encode and store the external signal.

Pareto optimization. We perform a Pareto optimization at stationarity in the presence of a prolonged stimulation. We seek the optimal values of (β, σ) by maximizing the functional

$$\mathcal{L}(\beta, \sigma) = \gamma \frac{I_{U,H}(\beta, \sigma)}{\max(I_{U,H})} - (1 - \gamma) \frac{\delta Q_R(\beta, \sigma)}{\max(\delta Q_R)}$$

where $\gamma \in [0, 1]$. Hence, we maximize the information between the readout and the field, simultaneously minimizing the dissipation of the receptor induced by both the signal and feedback process, as discussed in the main text. The values are normalized since, in principle, they can span different orders of magnitudes. In the Supplementary Information, we detailed the derivation of the Pareto front and show that qualitatively similar results can be obtained for a 3-d Pareto-like surface obtained by maximizing also the feedback information, ΔI_f .

Recording of whole brain neuronal activity in zebrafish larvae. Acquisitions of the zebrafish brain activity were carried out in one *Elavl3:H2BGCaMP6s* larvae at 5 days post fertilization raised at 28°C on a 12 h light/12 h dark cycle according to the approval by the Ethical Committee of the University of Padua (61/2020

dal Maschio). The subject was embedded in 2 percent agarose gel and brain activity was recorded using a multiphoton system with a custom 3D volumetric acquisition module. Data were acquired at 30 frames per second covering an effective field of view of about $450 \times 900 \mu\text{m}$ with a resolution of 512×1024 pixels. The volumetric module acquires a volume of about 180 – 200 μm in thickness encompassing 30 planes separated by about 7 μm , at a rate of 1 volume per second, sufficient to track the slow dynamics associated with the fluorescence-based activity reporter GCaMP6s. Visual stimulation was presented in the form of a looming stimulus with 150s intervals, centered with the fish eye (see Supplementary Information). Neurons identification and anatomical registrations were performed as described in [63].

Data analysis. The acquired temporal series were first processed using an automatic pipeline, including motion artifact correction, temporal filtering with a 3s rectangular window, and automatic segmentation. The obtained dataset was manually curated to resolve segmentation errors or to integrate cells not detected automatically. We fit the activity profiles of about 55000 cells with a linear regression model using a set of base functions representing the expected responses to each stimulation event. These base functions have been obtained by convolving the exponentially decaying kernel of the GCaMP signal lifetime with square waveforms characterizing the presentation of the corresponding visual stimulus. The resulting score coefficients of the fit were used to extract the cells whose score fell within the top 5% of the distribution, resulting in a population of ≈ 2400 neurons whose temporal activity profile correlates most with the stimulation protocol. The resulting fluorescence signals $F^{(i)}$ were processed by removing a moving baseline to account for baseline drifting and fast oscillatory noise [69]. See Supplementary Information.

Model for neural activity. Here, we describe how our framework is modified to mimic neural activity. Each readout unit, u , is interpreted as a population of N neurons, i.e., a region dedicated to the sensing of a specific input. Storage can be implemented, for example, as an inhibitory neural population, in line with recent observations in [15]. When a readout population is activated at time t , each of its N neurons fires with a probability p . We set $N = 100$ and $p = 0.5$. N has been set to have the same number of observed neurons in data and simulations, while p only controls the dispersal of the points in Fig. 5c, thus not altering the main message. The dynamics of each readout unit follows our dynamical model. Due to habituation, some of the readout units activated by the first stimulus will not be activated by subsequent stimuli. Although the evoked neural response cannot be captured by this extremely simple model, its archetypal ingredients (dissipation, storage, and feedback) are informative enough to reproduce the low-dimensional habituation dynamics found in experimental data.

-
- [1] G. Tkačik and W. Bialek, Information processing in living systems, *Annual Review of Condensed Matter Physics* **7**, 89 (2016).
- [2] E. U. Azeloglu and R. Iyengar, Signaling networks: information flow, computation, and decision making, *Cold Spring Harbor perspectives in biology* **7**, a005934 (2015).
- [3] F. S. Gnesotto, F. Mura, J. Gladrow, and C. P. Broedersz, Broken detailed balance and non-equilibrium dynamics in living systems: a review, *Reports on Progress in Physics* **81**, 066601 (2018).
- [4] I. Nemenman, Information theory and adaptation, *Quantitative biology: from molecular to cellular systems* **4**, 73 (2012).
- [5] T. Nakajima, Biologically inspired information theory: Adaptation through construction of external reality models by living systems, *Progress in Biophysics and Molecular Biology* **119**, 634 (2015).
- [6] M. Whiteley, S. P. Diggle, and E. P. Greenberg, Progress in and promise of bacterial quorum sensing research, *Nature* **551**, 313 (2017).
- [7] T. J. Perkins and P. S. Swain, Strategies for cellular decision-making, *Molecular systems biology* **5**, 326 (2009).
- [8] D. E. Koshland Jr, A. Goldbeter, and J. B. Stock, Amplification and adaptation in regulatory and sensory systems, *Science* **217**, 220 (1982).
- [9] Y. Tu, T. S. Shimizu, and H. C. Berg, Modeling the chemotactic response of escherichia coli to time-varying stimuli, *Proceedings of the National Academy of Sciences* **105**, 14855 (2008).
- [10] Y. Tu, The nonequilibrium mechanism for ultrasensitivity in a biological switch: Sensing by maxwell's demons, *Proceedings of the National Academy of Sciences* **105**, 11737 (2008).
- [11] H. Mattingly, K. Kamino, B. Machta, and T. Emonet, Escherichia coli chemotaxis is information limited, *Nature Physics* **17**, 1426 (2021).
- [12] R. Cheong, A. Rhee, C. J. Wang, I. Nemenman, and A. Levchenko, Information transduction capacity of noisy biochemical signaling networks, *science* **334**, 354 (2011).
- [13] H. Wajant, K. Pfizenmaier, and P. Scheurich, Tumor necrosis factor signaling, *Cell Death & Differentiation* **10**, 45 (2003).
- [14] E. Marquez-Legorreta, L. Constantin, M. Piber, I. A. Favre-Bulle, M. A. Taylor, A. S. Blevins, J. Giacomotto, D. S. Bassett, G. C. Vanwallegem, and E. K. Scott, Brain-wide visual habituation networks in wild type and *fmr1* zebrafish, *Nature Communications* **13**, 895 (2022).
- [15] H. Fotowat and F. Engert, Neural circuits underlying habituation of visually evoked escape behaviors in larval zebrafish, *Elife* **12**, e82916 (2023).
- [16] J. Benda, Neural adaptation, *Current Biology* **31**, R110 (2021).
- [17] G. Lan, P. Sartori, S. Neumann, V. Sourjik, and Y. Tu, The energy–speed–accuracy trade-off in sensory adaptation, *Nature physics* **8**, 422 (2012).
- [18] A. Menini, Calcium signalling and regulation in olfactory neurons, *Current opinion in neurobiology* **9**, 419 (1999).
- [19] A. Kohn, Visual adaptation: physiology, mechanisms, and functional benefits, *Journal of neurophysiology* **97**, 3155 (2007).
- [20] N. A. Lesica, J. Jin, C. Weng, C.-I. Yeh, D. A. Butts, G. B. Stanley, and J.-M. Alonso, Adaptation to stimulus contrast and correlations during natural visual stimulation, *Neuron* **55**, 479 (2007).
- [21] A. Benucci, A. B. Saleem, and M. Carandini, Adaptation maintains population homeostasis in primary visual cortex, *Nature neuroscience* **16**, 724 (2013).
- [22] E. Schneidman, M. J. Berry, R. Segev, and W. Bialek, Weak pairwise correlations imply strongly correlated network states in a neural population, *Nature* **440**, 1007 (2006).
- [23] G. Tkacik, O. Marre, D. Amodei, E. Schneidman, W. Bialek, and M. J. Berry, Searching for collective behavior in a large network of sensory neurons, *PLoS computational biology* **10**, e1003408 (2014).
- [24] Z. D. Kurtz, C. L. Müller, E. R. Miraldi, D. R. Littman, M. J. Blaser, and R. A. Bonneau, Sparse and compositionally robust inference of microbial ecological networks, *PLoS computational biology* **11**, e1004226 (2015).
- [25] K. Tunstrøm, Y. Katz, C. C. Ioannou, C. Huepe, M. J. Lutz, and I. D. Couzin, Collective states, multistability and transitional behavior in schooling fish, *PLoS computational biology* **9**, e1002915 (2013).
- [26] G. Nicoletti and D. M. Busiello, Mutual information disentangles interactions from changing environments, *Physical Review Letters* **127**, 228301 (2021).
- [27] G. Nicoletti and D. M. Busiello, Mutual information in changing environments: non-linear interactions, out-of-equilibrium systems, and continuously-varying diffusivities, *Physical Review E* **106**, 014153 (2022).
- [28] R. De Smet and K. Marchal, Advantages and limitations of current network inference methods, *Nature Reviews Microbiology* **8**, 717 (2010).
- [29] G. Nicoletti, A. Maritan, and D. M. Busiello, Information-driven transitions in projections of underdamped dynamics, *Physical Review E* **106**, 014118 (2022).
- [30] A. Celani, T. S. Shimizu, and M. Vergassola, Molecular and functional aspects of bacterial chemotaxis, *Journal of Statistical Physics* **144**, 219 (2011).
- [31] M. Kollmann, L. Løvdo, K. Bartholomé, J. Timmer, and V. Sourjik, Design principles of a bacterial signalling network, *Nature* **438**, 504 (2005).
- [32] W. H. de Ronde, F. Tostevin, and P. R. Ten Wolde, Effect of feedback on the fidelity of information transmission of time-varying signals, *Physical Review E* **82**, 031914 (2010).
- [33] J. Selimkhanov, B. Taylor, J. Yao, A. Pilko, J. Albeck, A. Hoffmann, L. Tsimring, and R. Wollman, Accurate information transmission through dynamic biochemical signaling networks, *Science* **346**, 1370 (2014).
- [34] N. Barkai and S. Leibler, Robustness in simple biochemical networks, *Nature* **387**, 913 (1997).
- [35] J. M. Parrondo, J. M. Horowitz, and T. Sagawa, Thermodynamics of information, *Nature physics* **11**, 131 (2015).
- [36] S. Flatt, D. M. Busiello, S. Zamuner, and P. De Los Rios, Abc transporters are billion-year-old maxwell demons, *Communications Physics* **6**, 205 (2023).
- [37] M. Bilancioni, M. Esposito, and N. Freitas, A chemical reaction network implementation of a maxwell demon, *The Journal of Chemical Physics* **159** (2023).

- [38] C. H. Bennett, The thermodynamics of computation — a review, *International Journal of Theoretical Physics* **21**, 905 (1982).
- [39] T. Sagawa and M. Ueda, Minimal energy cost for thermodynamic information processing: measurement and information erasure, *Physical review letters* **102**, 250602 (2009).
- [40] D. Hartich, A. C. Barato, and U. Seifert, Nonequilibrium sensing and its analogy to kinetic proofreading, *New Journal of Physics* **17**, 055026 (2015).
- [41] M. Skoge, S. Naqvi, Y. Meir, and N. S. Wingreen, Chemical sensing by nonequilibrium cooperative receptors, *Physical review letters* **110**, 248102 (2013).
- [42] I. Lestas, G. Vinnicombe, and J. Paulsson, Fundamental limits on the suppression of molecular fluctuations, *Nature* **467**, 174 (2010).
- [43] S. J. Coultrap and K. U. Bayer, Camkii regulation in information processing and storage, *Trends in neurosciences* **35**, 607 (2012).
- [44] P. W. Frankland and S. A. Josselyn, In search of the memory molecule, *Nature* **535**, 41 (2016).
- [45] J. Lisman, H. Schulman, and H. Cline, The molecular basis of camkii function in synaptic and behavioural memory, *Nature Reviews Neuroscience* **3**, 175 (2002).
- [46] P. Sartori, L. Granger, C. F. Lee, and J. M. Horowitz, Thermodynamic costs of information processing in sensory adaptation, *PLoS computational biology* **10**, e1003974 (2014).
- [47] A. C. Barato, D. Hartich, and U. Seifert, Efficiency of cellular information processing, *New Journal of Physics* **16**, 103024 (2014).
- [48] T. E. Ouldridge, C. C. Govern, and P. R. ten Wolde, Thermodynamics of computational copying in biochemical systems, *Physical Review X* **7**, 021004 (2017).
- [49] E. Penocchio, F. Avanzini, and M. Esposito, Information thermodynamics for deterministic chemical reaction networks, *The Journal of Chemical Physics* **157** (2022).
- [50] S. J. Rahi, J. Larsch, K. Pecani, A. Y. Katsov, N. Mansouri, K. Tsaneva-Atanasova, E. D. Sontag, and F. R. Cross, Oscillatory stimuli differentiate adapting circuit topologies, *Nature methods* **14**, 1010 (2017).
- [51] D. Tadres, P. H. Wong, T. To, J. Moehlis, and M. Louis, Depolarization block in olfactory sensory neurons expands the dimensionality of odor encoding, *Science Advances* **8**, eade7209 (2022).
- [52] M. Jalaal, N. Schramma, A. Dode, H. de Maleprade, C. Raufaste, and R. E. Goldstein, Stress-induced dinoflagellate bioluminescence at the single cell level, *Physical Review Letters* **125**, 028102 (2020).
- [53] M. S. Malmierca, M. V. Sanchez-Vives, C. Escera, and A. Bendixen, Neuronal adaptation, novelty detection and regularity encoding in audition, *Frontiers in Systems Neuroscience* **8**, 10.3389/fnsys.2014.00111 (2014).
- [54] W. L. Shew, W. P. Clawson, J. Pobst, Y. Karimippanah, N. C. Wright, and R. Wessel, Adaptation to sensory input tunes visual cortex to criticality, *Nature Physics* **11**, 659 (2015).
- [55] W. Ma, A. Trusina, H. El-Samad, W. A. Lim, and C. Tang, Defining network topologies that can achieve biochemical adaptation, *Cell* **138**, 760 (2009).
- [56] P. De Los Rios and A. Barducci, Hsp70 chaperones are non-equilibrium machines that achieve ultra-affinity by energy consumption, *Elife* **3**, e02218 (2014).
- [57] R. D. Astumian, Kinetic asymmetry allows macromolecular catalysts to drive an information ratchet, *Nature communications* **10**, 3837 (2019).
- [58] J. Yan, A. Hilfinger, G. Vinnicombe, J. Paulsson, *et al.*, Kinetic uncertainty relations for the control of stochastic reaction networks, *Physical review letters* **123**, 108101 (2019).
- [59] A. Hilfinger, T. M. Norman, G. Vinnicombe, and J. Paulsson, Constraints on fluctuations in sparsely characterized biological systems, *Physical review letters* **116**, 058101 (2016).
- [60] G. Nicoletti and D. M. Busiello, Information propagation in multilayer systems with higher-order interactions across timescales, *Physical Review X* **14**, 021007 (2024).
- [61] V. Ngampruetikorn, D. J. Schwab, and G. J. Stephens, Energy consumption and cooperation for optimal sensing, *Nature communications* **11**, 1 (2020).
- [62] L. F. Seoane and R. Solé, Phase transitions in pareto optimal complex networks, *Physical Review E* **92**, 032807 (2015).
- [63] M. Bruzzone, E. Chiarello, M. Albanesi, M. E. Miletto Petrazzini, A. Megighian, C. Lodovichi, and M. Dal Maschio, Whole brain functional recordings at cellular resolution in zebrafish larvae with 3d scanning multiphoton microscopy, *Scientific reports* **11**, 11048 (2021).
- [64] L.-A. Lamiré, M. Haesemeyer, F. Engert, M. Granato, and O. Randlett, Inhibition drives habituation of a larval zebrafish visual response, *bioRxiv*, 2022 (2022).
- [65] J. Hidalgo, J. Grilli, S. Suweis, M. A. Munoz, J. R. Banavar, and A. Maritan, Information-based fitness and the emergence of criticality in living systems, *Proceedings of the National Academy of Sciences* **111**, 10095 (2014).
- [66] D. M. Busiello, D. Gupta, and A. Maritan, Coarse-grained entropy production with multiple reservoirs: Unraveling the role of time scales and detailed balance in biology-inspired systems, *Physical Review Research* **2**, 043257 (2020).
- [67] S. Bo and A. Celani, Multiple-scale stochastic processes: decimation, averaging and beyond, *Physics reports* **670**, 1 (2017).
- [68] J. Schnakenberg, Network theory of microscopic and macroscopic behavior of master equation systems, *Reviews of Modern physics* **48**, 571 (1976).
- [69] H. Jia, N. L. Rochefort, X. Chen, and A. Konnerth, In vivo two-photon imaging of sensory-evoked dendritic calcium signals in cortical neurons, *Nature protocols* **6**, 28 (2011).